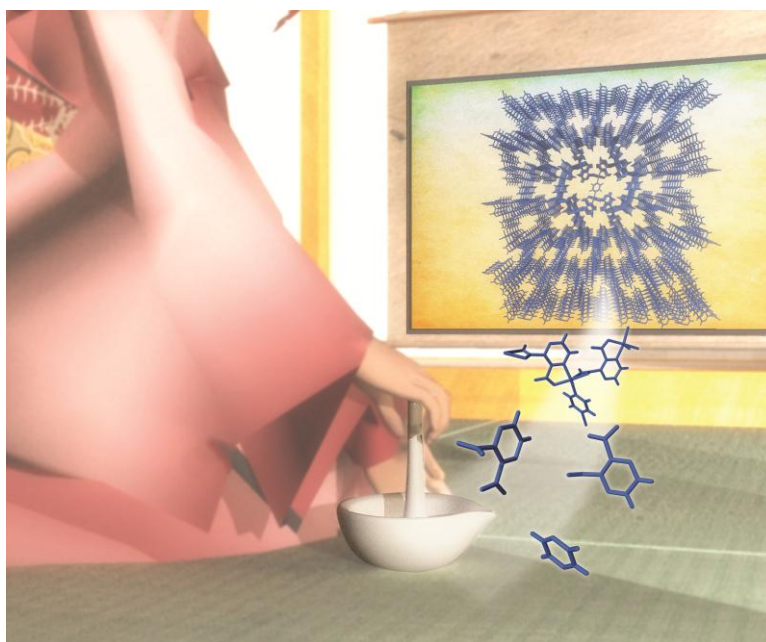


This article is published as part of the *Dalton Transactions* themed issue entitled:

Coordination chemistry in the solid state

Guest Editor Russell E. Morris

Published in [Issue 14, Volume 41](#) of *Dalton Transactions*



Articles in this issue include:

Communications

[Highly oriented surface-growth and covalent dye labeling of mesoporous metal–organic frameworks](#)

Florian M. Hinterholzinger, Stefan Wuttke, Pascal Roy, Thomas Preuße, Andreas Schaate, Peter Behrens, Adelheid Godt and Thomas Bein

Papers

[Supramolecular isomers of metal–organic frameworks: the role of a new mixed donor imidazolate-carboxylate tetradentate ligand](#)

Victoria J. Richards, Stephen P. Argent, Adam Kewley, Alexander J. Blake, William Lewis and Neil R. Champness

[Hydrogen adsorption in the metal–organic frameworks \$\text{Fe}_2\(\text{dobdc}\)\$ and \$\text{Fe}_2\(\text{O}_2\)\(\text{dobdc}\)\$](#)

Wendy L. Queen, Eric D. Bloch, Craig M. Brown, Matthew R. Hudson, Jarad A. Mason, Leslie J. Murray, Anibal Javier Ramirez-Cuesta, Vanessa K. Peterson and Jeffrey R. Long

Visit the *Dalton Transactions* website for the latest cutting inorganic chemistry

www.rsc.org/publishing/journals/dt/

Luminescent microporous metal–metallo salen frameworks with the primitive cubic net†

Chengfeng Zhu, Weimin Xuan and Yong Cui*

Received 22nd August 2011, Accepted 4th October 2011

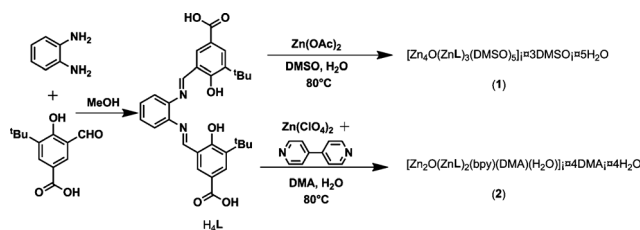
DOI: 10.1039/c1dt11584g

Two microporous three-dimensional metal–metallo salen frameworks are constructed from a dicarboxyl-functionalized Schiff base ligand and their H₂, CO₂ and CH₄ adsorption capacities and fluorescence quenching behavior to the vapor of nitroaromatic compounds are studied.

Metal–organic frameworks (MOFs) have attracted growing interest because of their intriguing architectures and topologies and promising applications in diverse areas such as gas storage, catalysis and separation.¹ Diversity of organic ligands and metal clusters such as dinuclear, trinuclear and tetranuclear and even higher-nuclear clusters have been utilized as secondary building blocks (SBUs) to make robust and porous MOFs.² In particular, combinations of 6-connected [Zn₄(μ₄-O)(O₂CR)₆] SBUs and 2-connected linear dicarboxylate bridging ligands of different lengths have produced a family of well-established isorecticular MOFs, which exhibited tunable pore and/or channel sizes, shapes and functionalities. Nevertheless, it remains a great challenge to further functionalize the Zn₄O-based isorecticular porous network materials.³

Metallo salen complexes [salen = *N,N'*-ethylenebis(salicylidene aminato)] have potential applications in homogenous catalysis and separation,⁴ but less attention has been given to assembling metallo salens into crystalline infinite solids.⁵ Recently, we reported the self-assembly of porous metal–organic crystalline materials from pyridyl/carboxyl-functionalized metallo salen complexes and showed their ability to selectively adsorb small organic molecules.^{4,6} We report here the synthesis of a dicarboxyl-functionalized Schiff base ligand to build two 3D microporous metal–metallo salen frameworks and their H₂, CO₂ and CH₄ adsorption capacities and fluorescence quenching behavior.

As outlined in Scheme 1, the dicarboxyl-functionalized salen ligand 1,2-phenyldiamine-*N,N'*-bis(3-*tert*-butyl-5-(carboxyl)-salicylidene) (H₄L) was synthesized in good yield by the 1 : 1 condensation of *o*-phenyldiamine with 3-*tert*-butyl-5-formyl-4-hydroxybenzoic acid. The ligand was characterized by ¹H

Scheme 1 Synthesis of H₄L, **1** and **2**.

and ¹³C NMR spectroscopies and ESI mass spectrometry (Fig. S12†). Heating Zn(OAc)₂·4H₂O and H₄L (2 : 1 molar ratio) in dimethyl sulfoxide (DMSO) and water at 80 °C afforded yellow block-like crystals [Zn₄O(ZnL)₃(DMSO)₅]·3DMSO·5H₂O (**1**) in good yield.‡ The products are all stable in air and insoluble in water and common organic solvents. The formula of **1** was determined by single-crystal X-ray diffraction studies, elemental analysis, IR spectroscopy and thermogravimetric analysis (TGA).

A single-crystal X-ray diffraction study performed on **1** reveals a neutral 3D open metal–organic network with the primitive cubic net.§ **1** crystallizes in the monoclinic space group *P*2₁/*n* and the asymmetric unit contains one formula unit. In the ZnL ligand, each Zn center adopts a square-pyramidal geometry with the equatorial plane occupied by one N₂O₂ donors of one L ligand and the apical position by one oxygen atom of a DMSO molecule (Fig. S1†). The Zn–N and Zn–O bond lengths range from 2.045 (6) to 2.123(6) Å and from 1.944(6) to 1.993(4) Å, respectively, while the zinc centers are located 0.451, 0.437 and 0.433 Å above the plane formed by N₂O₂ coordination toward the axial direction. Four Zn²⁺ ions form a tetranuclear Zn₄O cluster around a μ₄-O atom (Fig. 1). Of the four metal ions, three adopt a distorted tetrahedral geometry by coordinating to a μ₄-O atom and three carboxylate oxygen atoms from three ZnL metallo ligands and the fourth adopts a distorted octahedral geometry by coordinating to a μ₄-O atom, three carboxylate oxygen atoms and two DMSO molecules. The Zn–O bond distances vary from 1.913(2) to 2.006 (2) Å, and the adjacent Zn···Zn distances range from 3.082 to 3.281 Å, which are in the usual range for similar clusters.³

Each Zn₄O cluster in **1**, acting as a 6-connecting octahedral building unit, is thus linked by six ZnL units and each ZnL unit is linked to two Zn₄O units to create a 3D structure and the topology of **1** can be best described as a primitive cubic (α-Po) net (Fig. 2a, 2b). The single network possesses a large parallelogram channel with diagonal distances of ~19.2 × 31.2 Å along the

School of Chemistry and Chemical Technology and State Key Laboratory of Metal Matrix Composites, Shanghai Jiao Tong University, Shanghai, 200240, China. E-mail: yongcui@sjtu.edu.cn; Fax: (+86) 21-5474-1297

† Electronic supplementary information (ESI) available: Details of the synthetic procedures, spectra data and crystallographic data. CCDC reference numbers 787816 for **1** and 840526 for **2**, respectively. For ESI and crystallographic data in CIF or other electronic format see DOI: 10.1039/c1dt11584g

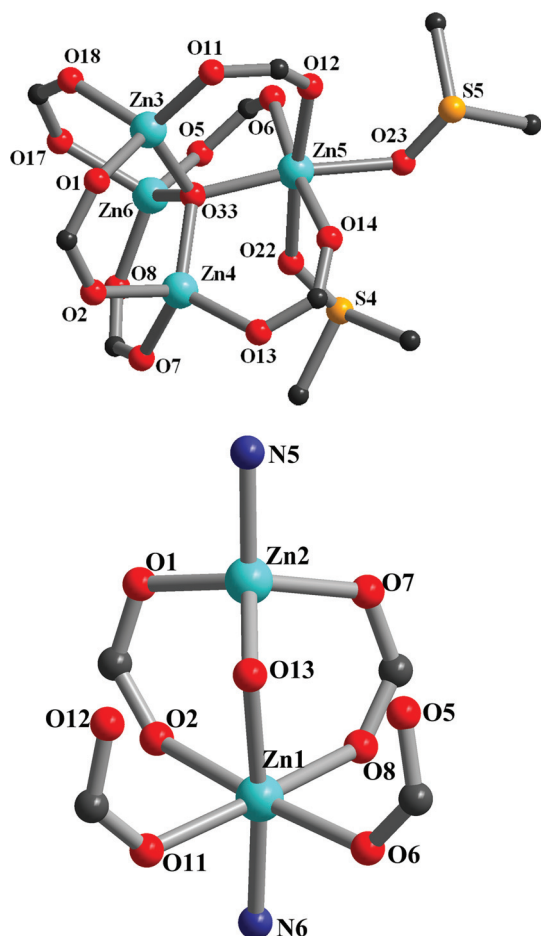


Fig. 1 View of the tetranuclear $[\text{Zn}_4\text{O}_6(\text{DMSO})_2]$ (top) and dinuclear $\text{Zn}_2\text{O}(\text{CO}_2)_4$ (down) clusters in **1** and **2**, respectively. Atoms labelled gray, carbon; cerulean, zinc; red, oxygen; yellow, sulphur; blue, nitrogen.

b-axis. Eight Zn_4O clusters are engaged in a distorted porous cube with a cavity dimension of $19.8 \times 20.6 \times 20.9 \text{ \AA}$ (Fig. 2b). The overall structure of **1** is a pair of identical α -Po nets of $[\text{Zn}_4\text{O}(\text{ZnL})_3]$, which are mutually interpenetrated with each other to form a doubly interpenetrating 3D framework. The pores of **1** along the *b* direction are fully filled with ZnL units from another α -Po net, while the pores are significantly reduced by double interpenetration of the 3D frameworks. Overall, there exists a 1D channel of $5.1 \times 3.9 \text{ \AA}$ which are filled with guest molecules (Fig. 2c). Calculations using the PLATON program indicate that **1** has 51.6% of total volume that is accessible for solvent molecules.⁷

A solvothermal reaction of $\text{Zn}(\text{ClO}_4)_2 \cdot 6\text{H}_2\text{O}$, 4,4'-bipyridine (bpy) and H_4L (a 2 : 1 : 1 molar ratio) in a mixture of dimethyl acetamide (DMA), water and triethylamine at $80 \text{ }^\circ\text{C}$ for 8 h afforded yellow strip-like crystals $[\text{Zn}_2\text{O}(\text{ZnL})_2(\text{bpy}) (\text{DMA}) (\text{H}_2\text{O})] \cdot 4\text{DMA} \cdot 4\text{H}_2\text{O}$ (**2**).[‡] The products are all stable in air and insoluble in water and common organic solvents. The formula of **2** was determined by single-crystal X-ray diffraction studies,[§] elemental analysis, IR and TGA.

The structure of **2** is constructed of dinuclear $\text{Zn}_2(\mu_2\text{-O})(\text{CO}_2)_4$ building blocks bridged by four ZnL units and bpy pillar linkers to form a 3D framework of a primitive cubic net (Fig. 3a,

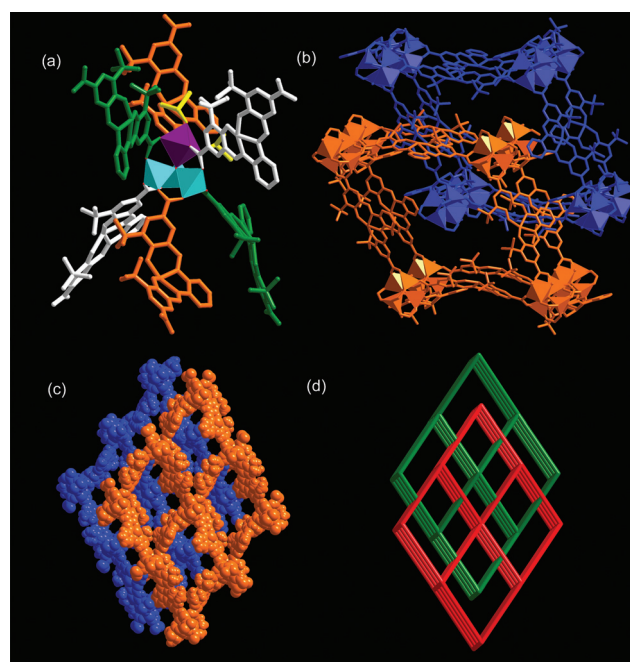


Fig. 2 Structure of **1** showing (a) the coordination geometry of the tetranuclear $\text{Zn}_4\text{O}(\text{CO}_2)_6$ building unit (H atoms are omitted for clarity); (b) two interpenetrated primitive cubic nets, and space-filling representations of (c) a 1D channel of $5.1 \times 3.9 \text{ \AA}$; (d) schematic illustration of the doubly interpenetrating frameworks in purple and green (the Zn_4O cluster is simplified as a node).

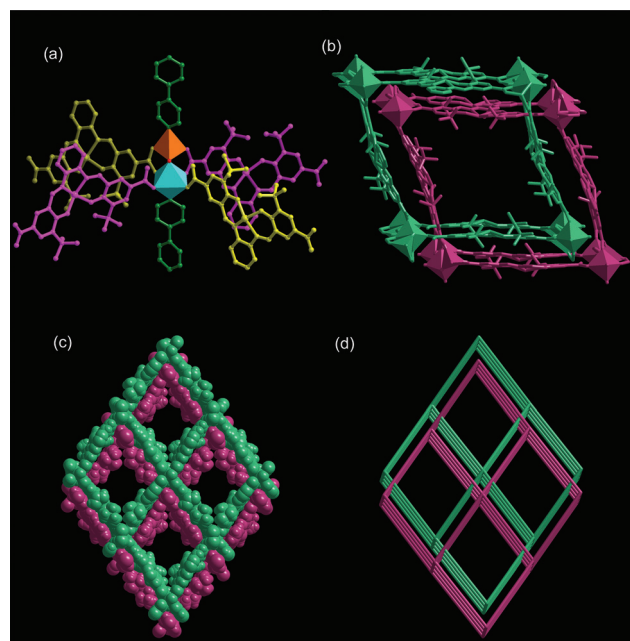


Fig. 3 Structure of **2** showing (a) the coordination geometry of the dinuclear $\text{Zn}_2\text{O}(\text{CO}_2)_4$ building unit (H atoms are omitted for clarity); (b) two interpenetrated primitive cubic nets, and space-filling representations of (c) a 1D channel of $13.4 \times 12.1 \text{ \AA}$; (d) schematic illustration of the doubly interpenetrating frameworks in purple and green (center of the dinuclear $\text{Zn}_2\text{O}(\text{CO}_2)_4$ as node).

3b). **2** also crystallizes in the monoclinic space group $P2_{(1)/n}$ and the asymmetric unit contains one formula unit. Each Zn center

in the two crystallographically independent ZnL units adopts a similar square-pyramidal geometry to that in **1**. In the dinuclear Zn₂O motif, the Zn1 adopts a distorted octahedron by coordination to a μ_2 -O atom, four carboxylate oxygen atoms from four metallosalens and one nitrogen atom from four bpy molecules, while Zn2 adopts a distorted tetrahedron by coordination to a μ_2 -O atom, two carboxylate oxygen atoms from two metallosalens and one nitrogen atom from the bpy molecule (Fig. 1). Thus, the dinuclear Zn₂O motif is linked by four ZnL units to form a 2D sheet that are further pillared by 4,4'-bipyridine to create a 3D structure with a primitive cubic net, which possesses a large parallelogram channel with diagonal distances of $\sim 23.0 \times 31.2$ Å similar to **1** along the *b*-axis, but with shorter diagonal distances of $\sim 21.3 \times 27.6$ Å along the *a*-axis due to the shorter bpy pillar compared with the dicarboxylate ZnL unit. Although the overall structure of **2** is a pair of identical α -Po nets of [Zn₂O(ZnL)₂-(bpy)], which are mutually interpenetrated with each other to form a doubly interpenetrating 3D framework (Fig. 3b), there still exists a larger 1D channel of 13.4×12.1 Å along the *b* axis (Fig. 3c). Calculations using the PLATON program indicate that **2** has 43.7% of the total volume that is accessible for solvent molecules.

The phase purity of both **1** and **2** were supported by the powder X-ray diffraction (XRD) pattern of the bulk sample, which are consistent with the calculated patterns (Fig. S11†). TGA shows that **1** loses 11.3% of its total weight upon heating to 200 °C, which corresponds to the loss of five water and three DMSO guest molecules per formula unit (calcd 11.8%) and the framework is stable up to 400 °C (Fig. S9†). While **2** loses 8.4% of its total weight upon heating to 175 °C, corresponding to four waters and one DMA molecule per formula (calcd 21.4%). The weight losses of **2** estimated from the compositions obtained from the single crystal X-ray diffraction are different from those obtained by TGA, which might be due to some of the adsorbed guest molecules having already been washed by CH₂Cl₂ and evaporated during the drying process before TGA analysis. The TGA result shows that **2** is stable up to 425 °C. Powder XRD experiments indicate that the evacuated frameworks of **1** and **2** retain crystallinity, although several diffraction peaks of **1** shifted a little compared with the pristine sample owing to slightly structural distortion after evacuation.

The permanent porosity of **1** is confirmed by its N₂ adsorption isotherm at 77 K. After desolvation, **1** exhibits a Type-I sorption behavior, with a BET surface area of 112 m² g⁻¹ (Fig. S15†). Whereas **2** only exhibits surface adsorption with a BET surface area of 10 m² g⁻¹. High-pressure gas adsorption measurements were performed to investigate the H₂, CH₄ and CO₂ uptake capacities of **1** and **2** (Fig. 4). After activation at 100 °C under vacuum, **1** can take up 1.75 wt% (195 cm³ g⁻¹ STP) of hydrogen at 10 bar and 77 K, while **2** has a higher adsorption capacity and can take up 2.7 wt% (302 cm³ g⁻¹ STP) of hydrogen under the same conditions. The hydrogen sorption profiles show a type I isotherm curve with a steep uptake in the low-pressure region, indicative of a strong affinity of H₂ molecules toward pore surfaces.⁸ The H₂ adsorption property is comparable to other MOFs of moderate H₂ adsorption.⁹ At 273 K and 10 bar, the adsorption capacities of **1** for CO₂ and CH₄ are 4.4 wt% (22.6 cm³ g⁻¹ STP) and 1.2 wt% (16.6 cm³ g⁻¹ STP), respectively. And **2** can also take up 9.6 wt% (49.0 cm³ g⁻¹ STP) of CO₂ and 1.9 wt%

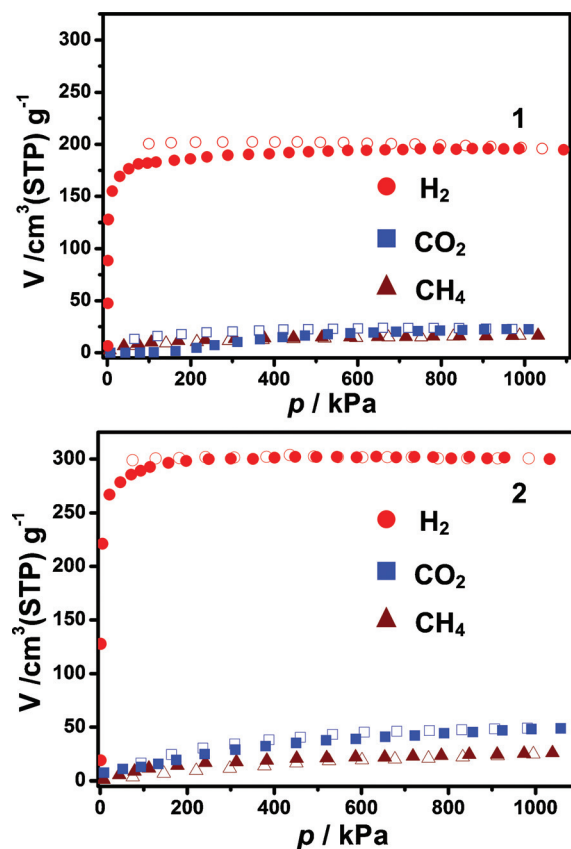


Fig. 4 The H₂, CO₂ and CH₄ adsorption isotherms of **1** and **2** (H₂: 77 K; CO₂: 273 K; CH₄: 273 K; closed symbols, adsorption; open symbols, desorption).

(25.9 cm³ g⁻¹ STP) of CH₄, respectively. The marked different uptake capacities for H₂, CH₄ and CO₂ indicate that they may hold potential for gas separation.¹⁰

(Salen)Zn complexes have been shown to exhibit fluorescence properties and accurately discriminated nitroaromatics.¹¹ This stimulates us to explore the utility of MOFs assembled from salen(Zn) in sensing nitroaromatics compounds that are highly explosive and environmentally deleterious. Fluorescence spectra were recorded on powder samples in thin-layer form, and it was found that compounds **1** and **2** emit strongly at 525 nm and 535 nm, respectively, upon excitation at 420 nm. To explore the applicability of the two frameworks for explosives detection, the fluorescence spectra of thin-layers were monitored, before and after exposing them to the vapors of nitroaromatics for varied periods of time (see Fig. 5). As expected, all nitroaromatics act as fluorescence quenchers for **1** and **2**. Among them, the most effective quencher is nitrobenzene (NB) compared with nitrotoluene (NT) and *m*-nitrotoluene (mNT). NB exhibits the strongest quenching effect not only because of its strongly electron-withdrawing -NO₂ group and the highest vapor pressure but also the absence of the electron-donating -CH₃ group.¹² Within ten seconds, NB quenches the emission by 44% and 67%, respectively, for **1** and **2**. After 4 min, the quenching percentages up to 58% and 75%, respectively. The quenching percentage (%) was simply estimated using the formula $(I_0 - I)/I_0 \times 100\%$, where I_0 is the original peak maximum intensity of the frameworks, I is the maximum intensity after exposure to the analyte. The thin

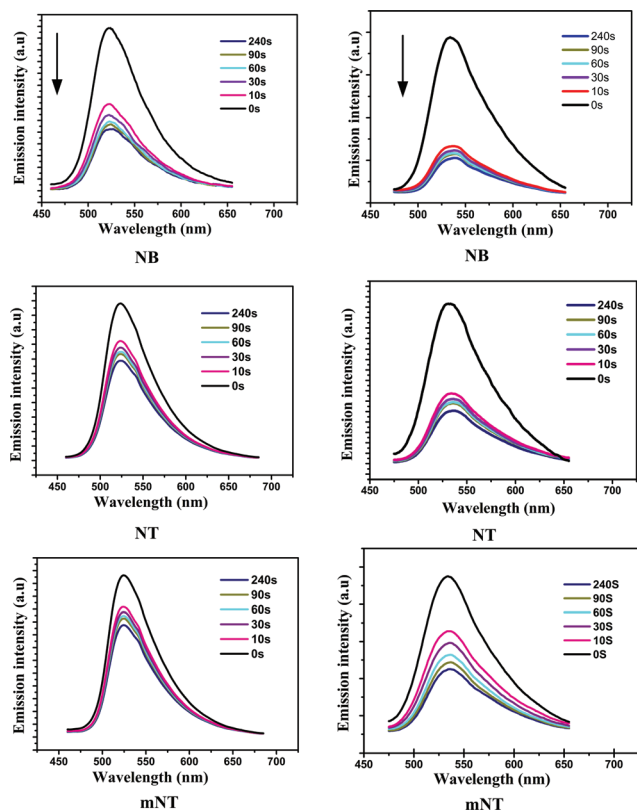


Fig. 5 Time-dependent fluorescence quenching by nitroaromatics before and after exposing **1** (left) and **2** (right) to the vapors of nitroaromatics for varied periods of time.

layer of **2** showed higher sensitivity toward nitroaromatic vapors than **1** films again, ascribed to the distinguished channels in **1** and **2**. We postulate that the larger open channel in **2** is more beneficial for the quenchers to diffuse into and to interact between the analyte and ZnL units. Fluorescence quenching is undergoing a mixed quenching pathway for ZnL. In the static process (ground-state process), a nonfluorescent QZnL adduct is forming in which the quencher binds to the ground-state of ZnL. And the dynamic quenching (excited-state process) comes from the quencher colliding with the excited state ZnL* through a bimolecular electron transfer from the phenolate ring of ZnL* to the nitroaromatics.¹³ However, no peak shift was observed in the quenching process, this means that the nitroaromatics do not interrupt the ligand-to-ligand charge transfers of the interpenetrating nets as observed in the crystal dynamic MOFs.¹⁴

In conclusion, we have synthesized and characterized two 2-fold interpenetrated 3D MOFs utilizing a dicarboxyl-functionalized Schiff-base ligand. The adsorption behaviors of the frameworks for H₂, CO₂ and CH₄ gases were investigated, and the fluorescence quenching behaviors upon exposure to the vapor of nitroaromatic compounds were studied.

Acknowledgements

This work was supported by NSFC-20971085 and 21025103, "973" Programs (2007CB209701 and 2009CB930403), STCSM-10DJ1400100 and the key project of MOE.

Notes and references

† Preparation of **1**: A mixture of Zn(OAc)₂·4H₂O (20.3 mg, 0.08 mmol) and H₄L (20.6 mg, 0.04 mmol) was placed in a small vial containing DMSO (5 mL) and H₂O (0.5 mL). The vial was sealed and heated at 80 °C for one day; yellow block-like crystals were collected, washed with methanol and acetone and dried in air. Yield: 19.8 mg (73.9% based on Zn). Elemental analysis (%) Calcd for C₁₀₆H₁₆₀N₆O₃₂S₈Zn₇: C 46.39, H 5.88, N 3.06, S 9.35. Found: C 46.25, H 5.84, N 3.03, S 9.40. IR (KBr): 3412(w), 3001(w), 2947(m), 2909(w), 1606(s), 1583(s), 1520(m), 1392(s), 1340(s), 1197(m), 1174(m), 1140(m), 1021(w), 800(w), 790(w), 753(w), 726(w), 706(w), 542(w) cm⁻¹. Preparation of **2**: A mixture of Zn(ClO₄)₂·6H₂O (29.6 mg, 0.08 mmol), 4, 4'-bipyridine (7.68 mg, 0.04 mmol) and H₄L (20.6 mg, 0.04 mmol) was placed in a small vial containing DMA (5 mL), H₂O (0.5 mL) and Et₃N (one drop). The vial was sealed and heated at 80 °C for 8 h; yellow strip-like crystals were collected, washed with dichloromethane and dried in air. Yield: 33.1 mg (85.0% based on Zn). Elemental analysis (%) Calcd for C₉₀H₁₂₈N₁₁O₂₁Zn₄: C 55.11, H 6.58, N 7.85. Found: C 55.20, H 6.53, N 7.82. IR (KBr): 3430(w), 3003(w), 2946(m), 2906(w), 1708(w), 1605(s), 1584(s), 1523(m), 1437(m), 1390(s), 1333(s), 1196(m), 1174(m), 1133(m), 1109(m), 1020(w), 934(w), 860(w), 790(w), 751(w), 726(w), 703(w), 639(w), 544(w), 500(w) cm⁻¹.

‡ Crystallographic data for **1**: *M* = 2401.86, monoclinic, space group *P*2₁/*n*, *a* = 22.286(2) Å, *b* = 19.845(2) Å, *c* = 34.290(4) Å, β = 90.968 (3)°, *V* = 15163(3) Å³, *Z* = 4, μ = 1.208 mm⁻¹, *D*_c = 1.052 Mg m⁻³, *F*(000) = 4952, 34348 unique (*R*_{int} = 0.1591), *R*₁ = 0.0752, *wR*₂ = 0.1597 [*I* > 2σ(*I*)], GOF = 1.028. The intensity data were collected on a Bruker Smart Apex II CCD diffractometer with graphite-monochromated Mo-Kα radiation (λ = 0.71073 Å) at 123 K. All absorption corrections were performed by using the SADABS program. The structure was solved by direct methods, and all non-H atoms were subjected to anisotropic refinement by full-matrix program. Contributions to scattering due to these highly disordered solvent molecules were removed using the SQUEEZE routine of PLATON;⁷ structures were then refined again using the data generated.

Crystallographic data for **2**: *M* = 1961.07, monoclinic, space group *P*2₁/*n*, *a* = 23.0013(6) Å, *b* = 14.0578(4) Å, *c* = 31.2380(8) Å, β = 90.881(2)°, *V* = 10099.5(5) Å³, *Z* = 4, μ = 1.648 mm⁻¹, *D*_c = 1.277 Mg m⁻³, *F*(000) = 4056, 10141 unique (*R*_{int} = 0.0420), *R*₁ = 0.1060, *wR*₂ = 0.2829 [*I* > 2σ(*I*)], GOF = 0.993. The intensity data were collected on a Bruker Smart Apex II CCD diffractometer with graphite-monochromated Cu-Kα radiation (λ = 1.54178 Å) at 123 K. All absorption corrections were performed by using the SADABS program. The structure was solved by direct methods, and all non-H atoms were subjected to anisotropic refinement by full-matrix program.

- (a) S. Kitagawa, R. Kitaura and S.-i. Noro, *Angew. Chem., Int. Ed.*, 2004, **43**, 2334; (b) G. Férey, *Chem. Soc. Rev.*, 2008, **37**, 191; (c) S.-C. Xiang, Z. Zhang, C.-G. Zhao, K. Hong, X. Zhao, D.-R. Ding, M.-H. Xie, C.-D. Wu, M. C. Das, R. Gill, K. M. Thomas and B. Chen, *Nat. Commun.*, 2011, **2**, 204; (d) M. C. Das, S. Xiang, Z. Zhang and B. Chen, *Angew. Chem. Int. Ed.*, 2011 n/a.
- (a) S. Ma, D. Sun, X.-S. Wang and H.-C. Zhou, *Angew. Chem., Int. Ed.*, 2007, **46**, 2458; (b) X. N. Cheng, W. X. Zhang, Y. Y. Lin, Y. Z. Zheng and X. M. Chen, *Adv. Mater.*, 2007, **19**, 1494; (c) M. Dincă, W. S. Han, Y. Liu, A. Dailly, C. M. Brown and J. R. Long, *Angew. Chem., Int. Ed.*, 2007, **46**, 1419; (d) Q.-R. Fang, G.-S. Zhu, Z. Jin, Y.-Y. Ji, J.-W. Ye, M. Xue, H. Yang, Y. Wang and S.-L. Qiu, *Angew. Chem., Int. Ed.*, 2007, **46**, 6638; (e) B. Luisi, Z. Ma and B. Moulton, *J. Chem. Crystallogr.*, 2007, **37**, 743.
- (a) L. Hou, Y. Y. Lin and X. M. Chen, *Inorg. Chem.*, 2008, **47**, 1346; (b) H. K. Chae, D. Y. Siberio-Perez, J. Kim, Y. Go, M. Eddaoudi, A. J. Matzger, M. O'Keefe and O. M. Yaghi, *Nature*, 2004, **427**, 523; (c) M. Eddaoudi, J. Kim, N. Rosi, D. Vodak, J. Wachter, M. O'Keefe and O. M. Yaghi, *Science*, 2002, **295**, 469.
- (a) G. Li, W. Yu and Y. Cui, *J. Am. Chem. Soc.*, 2008, **130**, 4582; (b) G. Li, W. Yu, J. Ni, T. Liu, Y. Liu, E. Sheng and Y. Cui, *Angew. Chem., Int. Ed.*, 2008, **47**, 1245.
- (a) S.-S. Sun, C. L. Stern, S. T. Nguyen and J. T. Hupp, *J. Am. Chem. Soc.*, 2004, **126**, 6314; (b) N. C. Gianneschi, P. A. Bertin, S. T. Nguyen, C. A. Mirkin, L. N. Zakharov and A. L. Rheingold, *J. Am. Chem. Soc.*, 2003, **125**, 10508; (c) F. Song, C. Wang, J. M. Falkowski, L. Ma and W. Lin, *J. Am. Chem. Soc.*, 2010, **132**, 15390.

- 6 (a) G. Yuan, C. Zhu, Y. Liu and Y. Cui, *Chem. Commun.*, 2011, **47**, 3180; (b) G. Yuan, C. Zhu, W. Xuan and Y. Cui, *Chem.–Eur. J.*, 2009, **15**, 6428.
- 7 A. Spek, *J. Appl. Crystallogr.*, 2003, **36**, 7.
- 8 B. Chen, X. Zhao, A. Putkham, K. Hong, E. B. Lobkovsky, E. J. Hurtado, A. J. Fletcher and K. M. Thomas, *J. Am. Chem. Soc.*, 2008, **130**, 6411.
- 9 (a) J. Luo, H. Xu, Y. Liu, Y. Zhao, L. L. Daemen, C. Brown, T. V. Timofeeva, S. Ma and H.-C. Zhou, *J. Am. Chem. Soc.*, 2008, **130**, 9626; (b) A. G. Wong-Foy, A. J. Matzger and O. M. Yaghi, *J. Am. Chem. Soc.*, 2006, **128**, 3494; (c) B. Chen, S. Ma, F. Zapata, E. B. Lobkovsky and J. Yang, *Inorg. Chem.*, 2006, **45**, 5718.
- 10 (a) L. J. Murray, M. Dincă and J. R. Long, *Chem. Soc. Rev.*, 2009, **38**, 1294; (b) J. R. Long and O. M. Yaghi, *Chem. Soc. Rev.*, 2009, **38**, 1213; (c) S. Ma and H.-C. Zhou, *Chem. Commun.*, 2010, **46**, 44.
- 11 (a) M. E. Germain and M. J. Knapp, *J. Am. Chem. Soc.*, 2008, **130**, 5422; (b) M. E. Germain, T. R. Vargo, P. G. Khalifah and M. J. Knapp, *Inorg. Chem.*, 2007, **46**, 4422.
- 12 S. Pramanik, C. Zheng, X. Zhang, T. J. Emge and J. Li, *J. Am. Chem. Soc.*, 2011, **133**, 4153.
- 13 M. E. Germain, T. R. Vargo, B. A. McClure, J. J. Rack, P. G. Van Patten, M. Odoi and M. J. Knapp, *Inorg. Chem.*, 2008, **47**, 6203.
- 14 (a) E. Y. Lee, S. Y. Jang and M. P. Suh, *J. Am. Chem. Soc.*, 2005, **127**, 6374; (b) D. Maspoch, D. Ruiz-Molina and J. Veciana, *Chem. Soc. Rev.*, 2007, **36**, 770.